

Resonant Raman scattering by LO phonons near the $E_0 + \Delta_0$ gap of GaSb

Wolfgang Kauschke and Manuel Cardona

*Max-Planck-Institut für Festkörperforschung, Heisenbergstrasse 1, 7000 Stuttgart 80,
Federal Republic of Germany*

(Received 13 November 1986)

We report on the resonance of Raman scattering by LO phonons near the $E_0 + \Delta_0$ gap of GaSb. Whereas the dipole-forbidden Fröhlich-induced scattering by LO phonons as well as the two-LO-phonon scattering are only seen at resonance, the weakly resonant dipole-allowed deformation potential-induced scattering by LO phonons dominates near the $E_0 + \Delta_0$ gap. The dipole-forbidden contribution is, however, clearly observed by means of its interference with the dipole-allowed scattering in the appropriate configurations. Absolute values for the Raman polarizabilities and efficiencies are displayed. A theoretical analysis yields the position of the $E_0 + \Delta_0$ gap and its Lorentzian broadening at 100 K, 1.549 ± 0.007 eV, and 6 ± 2 meV, respectively.

I. INTRODUCTION

In spite of possible applications, GaSb has not been as extensively studied as GaAs and InP. The band structure of GaSb near the Γ point is characterized by a small direct gap ($E_0 = 0.81$ eV at 2 K) and a large spin-orbit splitting ($\Delta_0 = 0.75$ eV). The conduction-band effective electron mass is very small ($m_e = 0.041m$) and the conduction-band minimum at the Γ point lies only 100 meV below that at the L point of the Brillouin zone. The E_1 and $E_1 + \Delta_1$ gaps along the Λ direction occur in the visible region ($E_1 = 2.16$ eV, $E_1 + \Delta_1 = 2.59$ eV).

Raman investigations on GaSb have especially dealt with resonance of optical-phonon scattering near the E_1 and $E_1 + \Delta_1$ gaps,¹⁻³ although cw dye lasers are available in the deep-red spectral region close to the $E_0 + \Delta_0$ gap. Recently, Raman studies in GaSb/AlSb superlattices near the E_1 resonances were reported.⁴

Near the $E_0 + \Delta_0$ gap of zinc-blende-type semiconductors the theory of resonant Raman scattering by LO phonons has been well established⁵⁻⁹ and successfully applied to experimental data on GaAs,⁸ $\text{Cd}_x\text{Hg}_{1-x}\text{Te}$,⁹ and InP.¹⁰ The dipole-allowed scattering results either from the deformation-potential contribution, the short-range part of the electron-phonon interaction, or from the Fröhlich interaction, the long-range part due to the electrical field of the LO phonon, via *interband* matrix elements (electro-optic contribution). Two mechanisms are involved in the dipole-forbidden Raman scattering by LO phonons, acting when the polarizations of the incident and scattered light are parallel to each other. The intrinsic mechanism arises from the *intraband* matrix elements of the Fröhlich electron-phonon interaction taking the q dependence of these matrix elements into account. The extrinsic impurity-induced scattering by LO phonons involves, in addition to the Fröhlich electron-phonon interaction, the elastic scattering of electrons (holes) by ionized impurities in fourth-order perturbation theory.^{11,12} Its scattering efficiency becomes comparable with that for intrinsic forbidden Raman scattering by LO phonons since momentum conservation is relaxed in this process

and larger q vectors enhance the scattering efficiency. The intrinsic dipole-forbidden contribution to the Raman scattering by LO phonon has been shown to interfere with the dipole-allowed one in GaAs (Refs. 8 and 13) and InP (Ref. 10). In this manner it can be distinguished from the extrinsic impurity-induced Raman scattering by LO phonons. The second-order resonant Raman scattering by LO phonons is formally similar to the impurity-induced one-phonon scattering;^{6,9} the electron-impurity interaction must be simply replaced by the Fröhlich intraband interaction. The Raman scattering by two LO phonons follows the selection rule of dipole-forbidden scattering. The fitting procedure adopted in Ref. 10 has shown that the most accurate information about the gap position and broadening is obtained from the two-LO-phonon resonance. These parameters can be used to fit the resonances and interferences for Raman scattering by one LO phonon, which are less sensitive to the broadening.

Here we apply this fitting procedure to experimental data obtained for bulk p -type, unintentionally doped GaSb near the $E_0 + \Delta_0$ gap. In a brief theoretical part we will summarize the notation and concepts important to this paper as well as essential features of the different scattering mechanisms by LO phonons necessary to elucidate the discussion. For detailed expressions the reader is referred to Refs. 8-10.

II. THEORY

The scattering intensities for Raman scattering by LO phonons are displayed either as squared Raman polarizabilities $|\hat{\mathbf{e}}_S \cdot \vec{\mathbf{R}} \cdot \hat{\mathbf{e}}_L|^2$ or as Raman scattering efficiencies $dS/d\Omega$ (per unit length and unit solid angle Ω). In the case of Raman scattering by one LO phonon they can be converted into each other by⁸

$$\frac{dS}{d\Omega} \Big|_{\text{LO}} = \frac{\omega_S^3 \omega_L}{c^4} \frac{\hbar}{2V_c M^* \Omega_{\text{LO}}} \frac{n_S}{n_L} \times |\hat{\mathbf{e}}_S \cdot \vec{\mathbf{R}} \cdot \hat{\mathbf{e}}_L|^2 [n(\Omega_{\text{LO}}) + 1], \quad (1)$$

where ω_L (ω_S) is the frequency of the incident (scattered) light, c the speed of the light in vacuum, V_c the volume of the primitive cell, $M^* = (M_{\text{Ga}}^{-1} + M_{\text{Sb}}^{-1})^{-1}$ the reduced mass of the unit cell. Ω_{LO} denotes the frequency of the LO phonon, $n(\Omega_{\text{LO}})$ the phonon occupation number, n_L (n_S) the refractive index, and \hat{e}_L and \hat{e}_S are the polarization vectors of the incident and scattered light, respectively. \vec{R} is the Raman tensor with matrix elements a_{LO} , the so-called Raman polarizabilities. An expression similar to Eq. (1) holds for the Raman scattering by two LO phonons.⁹ The scattering efficiencies $dS/d\Omega$ as compared with the squared Raman polarizabilities, include the ω^4 law for dipole radiation as well as the dependence on the phonon occupation number.

Dipole-allowed scattering by LO phonons arises from the deformation-potential electron-phonon interaction and from the electrooptical contribution of the Fröhlich (interband) interaction. Its Raman tensor for backscattering at a (001) face is given by^{14,15}

$$\vec{R}_{\text{DP}} = \begin{pmatrix} 0 & a_{\text{DP}} & 0 \\ a_{\text{DP}} & 0 & 0 \\ 0 & 0 & 0 \end{pmatrix}. \quad (2)$$

The deformation-potential-induced Raman polarizability a_{DP} can be expressed as a function of two- or three-band contributions from different critical points, such as E_0 , $E_0 + \Delta_0$, E_1 , and $E_1 + \Delta_1$. For the detailed expression we refer to Eq. (4) of Ref. 10. It is important to note that near the $E_0 + \Delta_0$ gap no two-band terms are operative. Thus, the resonance enhancement is low for deformation-potential scattering at this critical point. The E_0 and $E_0 + \Delta_0$ gaps contribute real and imaginary parts to the Raman tensor \vec{R}_{DP} [coefficient A_1 in Eq. (4) of Ref. 10], whereas the $E_1 - E_1 + \Delta_1$ gaps (A_2), and higher gaps (A_3), corresponding to virtual transitions, yield only real terms. The coefficients A_1 and A_2 can be related to electron-phonon deformation potentials as shown in Eqs. (5) and (6) of Ref. 10.

The intrinsic dipole-forbidden Raman scattering by LO phonons results from the \mathbf{q} dependence of the intraband matrix elements of the Fröhlich electron-phonon interaction. It can be represented by a diagonal tensor \vec{R}_F with the Raman polarizability a_F . The dependence of a_F on the frequency of the laser light is given by Eq. (9) of Ref. 10. It is proportional to the Fröhlich constant:

$$C_F = [2\pi e^2(\epsilon_\infty^{-1} - \epsilon_0^{-1})\hbar\Omega_{\text{LO}}]^{1/2}, \quad (3)$$

where e is the free-electron charge, ϵ_∞ and ϵ_0 are the high- (ir) and low-frequency (rf) dielectric constants, which are related to the LO-TO-phonon splitting via the Lyddane-Sachs-Teller relation.¹⁶ The intrinsic Fröhlich-induced Raman scattering shows a resonance at all direct gaps. Its resonance near the $E_0 + \Delta_0$ gap is symmetric with respect to $E_0 + \Delta_0 + \hbar\Omega_{\text{LO}}/2$. The imaginary part of a_F can be obtained from its real part just by reflection through a mirror plane at $E_0 + \Delta_0 + \hbar\Omega_{\text{LO}}/2$, the real part

of a_F peaking at the lower-energy side (see, i.e., Fig. 8 of Ref. 10).

The deformation potential and the \mathbf{q} -dependent Fröhlich-induced scattering are coherent with each other, since they are intrinsic processes leading to the same final states in \mathbf{q} space. Their Raman tensors have to be added to account for the coherence of both processes.

The impurity-induced dipole-forbidden Raman scattering by LO phonons is of extrinsic nature. The final expression for the squared Raman polarizability $|a_{Fi}|^2$ derived from fourth-order perturbation theory, assuming scattering by ionized impurities, is given by Eq. (11) of Ref. 8. It resonates near the $E_0 + \Delta_0$ gap, when the energy of the incident (incoming) and scattered (outgoing) light equals the gap (Fig. 2 of Ref. 8), and leads to final states different from those of the intrinsic processes. Hence the intensity of impurity-induced dipole-forbidden scattering add incoherently to the intensity of intrinsic Raman scattering by LO phonons (\mathbf{q} -induced, deformation potential). The scattering intensity for these extrinsic processes is, as in the case of intrinsic dipole-forbidden Raman scattering, proportional to C_F^2 .

The expression for the resonance of Raman scattering by two LO phonons is given by Eqs. (2) and (7) of Ref. 9. It obeys the same selection rules as dipole-forbidden Raman scattering by one LO phonon ($\hat{e}_S \parallel \hat{e}_L$). From the iteration or two Fröhlich-type electron-phonon interactions a C_F^4 dependence of the Raman scattering efficiency results. Near the $E_0 + \Delta_0$ gap the Raman scattering by two LO phonons reveals one distinct peak at the outgoing resonance ($\hbar\omega_L = E_0 + \Delta_0 + 2\hbar\Omega_{\text{LO}}$). The position and the sharpness of this resonance is a very sensitive function of the position and the broadening of the electronic gap, thus suggesting that a fitting procedure for resonant Raman scattering by LO phonons and its interference should start with the two-LO-phonon resonance.¹⁰

III. EXPERIMENTAL DETAILS

A single-crystal ingot of GaSb was grown by the Czochralski technique without initial doping. The samples prepared from it were p type with an estimated impurities concentration $N_A + N_D \approx 10^{16} \text{ cm}^{-3}$. They were cut as slabs with a (001) face. We denote by x , y , z , x' , and y' the [100], [010], [001], [110], and $[\bar{1}\bar{1}0]$ directions of the crystal, respectively. The [110] and $[\bar{1}\bar{1}0]$ directions are physically inequivalent at a (001) face of a III-V compound. Using the earlier convention [the Ga atoms of (0,0,0); the Sb atoms at $(a_0/4)(1,1,1)$ (Ref. 8)], the $[\bar{1}\bar{1}\bar{1}]$ face, parallel to [110], is Ga terminated.⁸ The [110] and $[\bar{1}\bar{1}0]$ can be determined by inspection of the etch pattern developed by preferential etching.¹⁷ The Raman measurements were performed at liquid-nitrogen temperature ($\approx 100 \text{ K}$). Four different backscattering geometries at a (001) face were used in order to distinguish the dipole-forbidden and dipole-allowed scatterings by LO phonons and to separate the intrinsic \mathbf{q} -induced Fröhlich scattering from the extrinsic impurity-induced one.^{8,10} The squared Raman polarizability $|\hat{e}_S \cdot \vec{R} \cdot \hat{e}_L|^2$ in each configuration is given by

$$\begin{aligned}
\text{(I)} \quad \bar{z}(x',x')z: & \quad |a_F + a_{\text{DP}}|^2 + |a_{\text{Fi}}|^2, \\
\text{(II)} \quad \bar{z}(y',y')z: & \quad |a_F - a_{\text{DP}}|^2 + |a_{\text{Fi}}|^2, \\
\text{(III)} \quad \bar{z}(x,x)z: & \quad |a_F|^2 + |a_{\text{Fi}}|^2, \\
\text{(IV)} \quad \bar{z}(y,x)z: & \quad |a_{\text{DP}}|^2.
\end{aligned} \tag{4}$$

Configurations (I) and (II) yield the interference between the dipole-allowed and dipole-forbidden scattering by LO phonons. The difference between both configurations results from the fact that the Raman tensor \vec{R}_{DP} and \vec{R}_F have to be coherently added *before* squaring. The contribution from the extrinsic impurity-induced scattering by LO phonons, however, must be incoherently added *after* squaring. Configuration (III) shows the dipole-forbidden scattering by one LO phonon as well as its first overtone. Configuration (IV) gives the dipole-allowed Raman scattering by LO phonons, only.

We used the cw-dye laser with the dye LD700 (Lambda Physik, Göttingen) to excite the spectra. The dye was pumped with all red lines of a Kr^+ laser (4.5 W). It lased in the spectral range 1.5–1.7 eV, close to the $E_0 + \Delta_0$ gap of GaSb. The laser beam was focused onto the sample with a cylindrical lens, keeping the power density below 10 W/cm^2 .

We chose high-purity silicon as a reference in order to obtain absolute values for the Raman scattering efficiencies and the squared Raman polarizabilities by the sample-substitution method.¹⁵ We assumed $|a| = 30 \text{ \AA}^2$ for the optical phonon of Si near 1.6 eV ($dS/d\Omega = 2.2 \times 10^{-6} \text{ sr}^{-1} \text{ cm}^{-1}$).¹⁸ In the case of Raman scattering by one LO phonon, the counting rates R'_S outside the crystal were corrected for absorption, reflectivity, and refractive index according to⁸

$$R'_S = \left[\frac{T_S T_L [n(\Omega_{\text{ph}}) + 1]}{(\alpha_L + \alpha_S) n_S n_L M^* \Omega_{\text{ph}} V_c} \right] \frac{\Delta\Omega'}{2c^4} P'_L |\hat{\mathbf{e}}_S \cdot \vec{\mathbf{R}} \cdot \hat{\mathbf{e}}_L|^2. \tag{5}$$

α_L (α_S), T_L (T_S), and n_L (n_S) are the absorption coefficient, the power-transmission coefficient, and the refractive index at the frequency ω_L (ω_S) of the incident (scattered) light, respectively. $\Delta\Omega'$ and P'_L denote the collection solid angle and the power of the incident laser light *outside* the crystal; M^* the reduced mass of the primitive cell; V_c its volume, Ω_{ph} , $n(\Omega_{\text{ph}})$, and c the phonon frequency, phonon occupation number, and speed of light in vacuum, respectively.

The expression in large parentheses in Eq. (5) has to be applied as a correction factor when using the sample substitution method to obtain squared Raman polarizabilities. In order to perform this correction we use the absorption data on Si from Ref. 19 and those of GaSb from ellipsometric measurements ($\alpha \cong 6.8 \times 10^4 \text{ cm}^{-1}$ at 1.6 eV).²⁰ Other required values of optical constants were also taken from ellipsometric measurements.²⁰

IV. RESULTS AND DISCUSSION

Figures 1 and 2 depict the resonance curves for scattering by one and two LO phonons in the three different

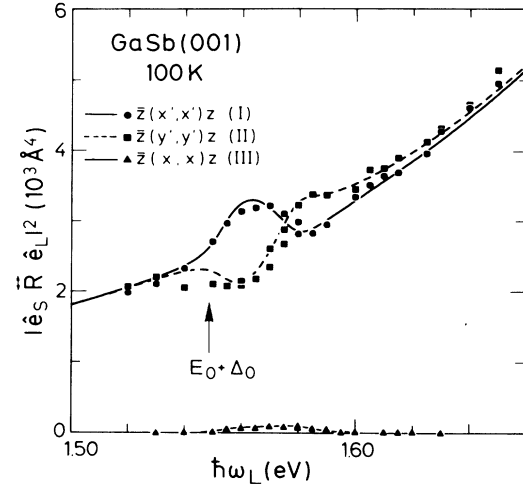


FIG. 1. Squared Raman polarizability of scattering by LO phonons near the $E_0 + \Delta_0$ gap of GaSb for three scattering configurations ($\hat{\mathbf{e}}_S \parallel \hat{\mathbf{e}}_L$). The lines are theoretical fits to the experimental curves (see text).

scattering configurations (I)–(III) near the $E_0 + \Delta_0$ gap of GaSb. In Fig. 1 the $\bar{z}(x',x')z$ configuration (I) yields the constructive interference. The intensity of dipole-allowed deformation-potential scattering (configuration IV, omitted in Fig. 1) follows the average of configurations I and II (the structure between 1.54 and 1.60 eV disappears). The dipole-forbidden scattering by LO phonons (III) is about a factor of 30 lower than the dipole-allowed one: it can only be seen near resonance. Its effect is, however, re-

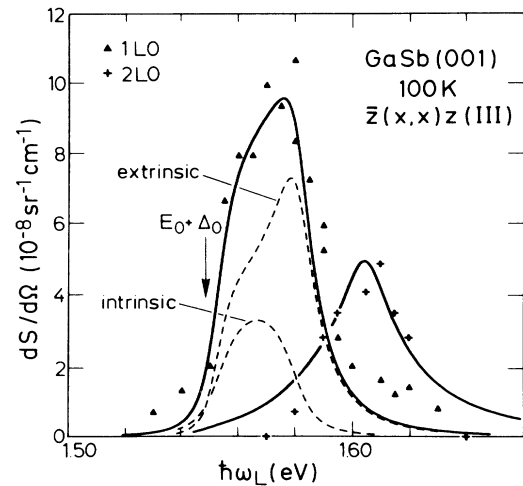


FIG. 2. Raman scattering efficiencies for one-LO and two-LO-phonon forbidden scattering near the $E_0 + \Delta_0$ gap of GaSb. The solid lines are fits to the experimental resonance curves. The dashed lines depict separately the intrinsic and extrinsic contributions to the forbidden Raman scattering by one LO phonon.

vealed by the interference with the dipole-allowed scattering (I and II). The scattering intensities of configurations I and II are nearly symmetrical with respect to that of configuration IV, a fact which indicates that only interfering cross terms between allowed and forbidden Raman scattering are important, any noninterfering forbidden contributions being negligible. The real part must be larger than the imaginary one, since towards the high-energy side of the resonance we observe a considerable enhancement due to the E_1 gap of GaSb. Virtual transitions above the energy under consideration only contribute a real part to the Raman tensor.

In Fig. 2 we have enlarged the lower part of Fig. 1 (triangles). The experimental data are displayed as scattering efficiencies $dS/d\Omega$, in order to compare dipole-forbidden Raman scattering by one and two LO phonons. The latter can only be detected very close to resonance, remaining even at resonance one-half smaller than the forbidden scattering by one LO phonon. This feature differs from that found in InP,¹⁰ Ga_{1-x}Al_xAs,²¹ and Cd_xHg_{1-x}Te.⁹ It can be understood qualitatively by the small ionicity of the Ga—Sb bonds.²² The Fröhlich constant C_F of GaSb calculated from the TO-LO phonon splitting [Eq. (3)] is about 3 times smaller than, e.g., in InP (see Table I in this paper and Table I of Ref. 10). It enters the Raman efficiency for forbidden scattering by one LO phonon as a square [Eqs. (9) and (A1) of Ref. 8] and that for two LO phonons as C_F^4 [Eq. (7) of Ref. 9].

The low intensity of the Raman scattering by two LO phonons renders the fit of the experimental data with the theoretical expressions (Ref. 10) more inaccurate. The best fit is obtained with the parameters of Table I. From the resonance of Raman scattering by two LO phonons we determine $E_0 + \Delta_0 = 1.546 \pm 0.004$ eV and $\eta = 6 \pm 2$ meV (right solid curve in Fig. 2). The Raman scattering by one LO phonon (interference in Fig. 1, dipole-

forbidden scattering in Fig. 2) yields $E_0 + \Delta_0 = 1.552 \pm 0.004$ eV and $\eta = 6 \pm 2$ meV (lines in Fig. 1, left curves in Fig. 2), which is compatible with the values obtained from two-LO-phonon scattering within the experimental error. The discrepancies between the experimental data and the theoretical curves are likely to be caused by the low Raman-scattering efficiency, in spite of the resonance. A small amount of DP scattering due to a slight sample misorientation or depolarization scattering may contribute to a small nonresonant background ($\sim 1 \times 10^{-8}$ sr⁻¹ cm⁻¹) in the case of one-LO-phonon dipole-forbidden scattering. On the other hand both features, the one- and two-LO-phonon lines, are difficult to distinguish from the background more than 20 meV away from resonance, thus defining a lower limit of sensitivity (about 1×10^{-8} sr⁻¹ cm⁻¹).

$E_0 + \Delta_0 = 1.549 \pm 0.007$ eV is consistent with results from stress-modulated magnetorefectance at 30 K (1.559 ± 0.002 eV).²⁵ The broadening η of the $E_0 + \Delta_0$ gap has been chosen to be 6 meV, 2 meV smaller than reported in Ref. 25; it is, however, at the upper limit of the error bars compatible with 8 meV obtained from magnetorefectance.²⁵ For $\eta = 6$ meV the calculated scattering efficiency for two LO phonons at the resonance maximum ($dS/d\Omega|_{\text{theor}} = 4.6 \times 10^{-8}$ sr⁻¹ cm⁻¹) equals that found experimentally ($dS/d\Omega|_{\text{expt}} = 4.5 \times 10^{-8}$ sr⁻¹ cm⁻¹). The agreement is perfect, but fortuitous, since we must take into account the total error of the measured Raman efficiency of GaSb (about 50%), considerable uncertainties of the parameters of Table I, and the neglect of excitonic interaction.

Following the analysis of Lawaetz³⁰ the broadening η can be related to the optical deformation potential d_0 : the broadening of $E_0 + \Delta_0$ is then mainly due to the lifetime of the hole in the split-off band. At low temperature the hole state in the split-off band decays into the heavy- and light-hole bands by emission of an optical phonon. Neglecting multiple coupling of phonons to holes, there is a nonpolar and polar contribution to the broadening η of the $E_0 + \Delta_0$ gap:³⁰

$$\eta = \xi_1 d_0^2 + \xi_p a_p^2. \quad (6)$$

$\xi_p a_p^2$, the broadening induced by the polar-optical coupling, amounts to 0.3 meV in GaSb, whereas the main part is due to the nonpolar deformation-potential interaction $\xi_1 d_0^2$.³⁰ The ξ 's are weighting factors which take the density of states and the \mathbf{k} space integration into account ($\xi_1 = 7.4 \times 10^{-6}$ eV⁻¹ for GaSb in Ref. 30). a_p describes the strength of the polar-optical coupling, and the optical deformation potential d_0 describes the nonpolar coupling. From Eq. (6) and $\eta = 6$ meV we obtain $d_0 = 28$ eV, whereas from the magnetorefectance value of $\eta = 8$ meV $d_0 = 32$ eV is obtained.³⁰ Within the experimental error these values agree well with $d_0 = 32$ eV calculated by the empirical pseudopotential method (EPM) and also the linear configuration of atomic orbitals (LCAO) method.³¹ However, the smaller broadening $\eta = 6$ meV obtained from resonant Raman scattering with respect to that from magnetorefectance ($\eta = 8$ meV) (Ref. 30) is consistent with the earlier observation in InP (Ref. 10) and

TABLE I. Parameters used to evaluate the theoretical expressions of the Raman polarizabilities in GaSb.

$E_0 = 0.81$ eV ^a	$E_1 = 2.16$ eV ^b
$E_0 + \Delta_0 = 1.549 \pm 0.005$ eV ^b	$E_1 + \Delta_1 = 2.59$ eV ^b
$\eta = 6 \pm 2$ meV ^b	$\hbar\Omega_{\text{LO}} = 29$ meV ⁱ
$m_e = 0.041 m^c$	$M^* = 81395 m^j$
$m_h = 0.13 m^d$	$a_0 = 6.08$ Å ^k
$P^2/m = 11.8$ eV ^e	$C_F = 1 \times 10^{-5}$ eV cm ^{-1/2} l
$q = 7.3 \times 10^5$ cm ⁻¹ f	$X_F = 0.06^m$

^aReference 23.

^bDetermined from the fit of the resonance curves.

^cReference 24.

^dReferences 23 and 25.

^eObtained from the effective masses using $\mathbf{k} \cdot \mathbf{p}$ theory.

^f $(n_L \omega_L + n_S \omega_S)/c$.

^gReference 26.

^hReference 27.

ⁱReference 28.

^j $M^* = (M_{\text{Ga}}^{-1} + M_{\text{Sb}}^{-1})^{-1}$.

^kReference 29.

^lSee Eq. (3).

^mSee definition in Ref. 8.

$\text{Al}_x\text{Ga}_{1-x}\text{As}$ (Ref. 21) that the broadening obtained from Raman scattering are always lower than those from modulation spectroscopy. The same conclusion holds for the optical deformation potentials d_0 determined from these broadenings.

The solid curve on the left side of Fig. 2 represents a fit to the dipole-forbidden Raman scattering by LO phonons assuming a contribution from the intrinsic \mathbf{q} -dependent and extrinsic impurity-induced Fröhlich scattering. Both contributions are depicted in Fig. 2 as dashed lines. The best fit of the LO-phonon interference in Fig. 1 (solid and dashed lines) is found for a $(30 \pm 7)\%$ intrinsic contribution, measured by the relative strength of the squared Raman polarizability of the intrinsic contribution with respect to that of the total forbidden scattering by LO phonons

$$|a_F|_{\max}^2 / (|a_F|_{\max}^2 + |a_{Fi}|_{\max}^2),$$

with

$$|a_F|_{\max}^2 = 0.4 |a_{Fi}|_{\max}^2.$$

The relative contribution of the intrinsic forbidden scattering is somewhat lower than in high-purity InP (Ref. 10) and GaAs (Refs. 8 and 21) epitaxial samples. It is comparable to an ionized impurity concentration $N_A - N_D \cong 10^{15} \text{ cm}^{-3}$, measured for the ingot at 78 K. The screening parameter $x_F = 0.06$ (for definition see Ref. 8) corresponds to an impurity concentration of about $2 \times 10^{14} \text{ cm}^{-3}$ when interpreted as one-half of the mean distance between impurities.

The fit of the dipole-allowed deformation potential scattering in Fig. 1 has been obtained using Eq. (4) of Ref. 10 with $A_1 = 7$, $A_2 = 50$, and $A_3 = -100$ and the parameters of Table I. Figure 3 displays the real and imaginary parts of the Raman polarizabilities a_{DP} and a_F for deformation-potential and intrinsic Fröhlich-induced scattering by one LO phonon. The relative signs of A_1 , A_2 , and A_3 are found to be the same as for GaAs (Refs. 8, 14, and 21) and InP (Ref. 10). To account for the enhancement towards the high-energy side of the resonance (Fig. 1) the real part of a_{DP} must be chosen much larger than the imaginary one. For this reason A_2 due to the E_1 and $E_1 + \Delta_1$ gaps has to be increased with respect to A_1 ($E_0 + \Delta_0$ contribution). The real part A_3 due to higher gaps compensates A_2 on the low-energy side of Fig. 1 to fit absolute values. The final result is rather insensitive to the exact value of A_1 . We chose the contribution of the $E_0 - E_0 + \Delta_0$ gaps, $A_1 = 7$, as for GaAs.^{14,21} The parameter A_1 (in \AA^2) can be expressed as a function of the deformation potential d_0 of the $E_0 - E_0 + \Delta_0$ gap:^{10,14}

$$A_1 = \frac{\sqrt{3}}{128\pi} \frac{a_0^2}{E_0} C_0'' d_0, \quad (7)$$

where a_0 is the lattice constant, E_0 the energy of the E_0 gap, and C_0'' a constant deduced from the piezobirefringence for [111] stress.³² We obtain $C_0'' d_0 = 35 \text{ eV}$. Experimental values for C_0'' of GaSb can be found in the literature: $C_0'' = 2.5 - 6.7$.³² The determination of C_0'' implies large uncertainties. C_0'' between 2.5 and 6.7 yields

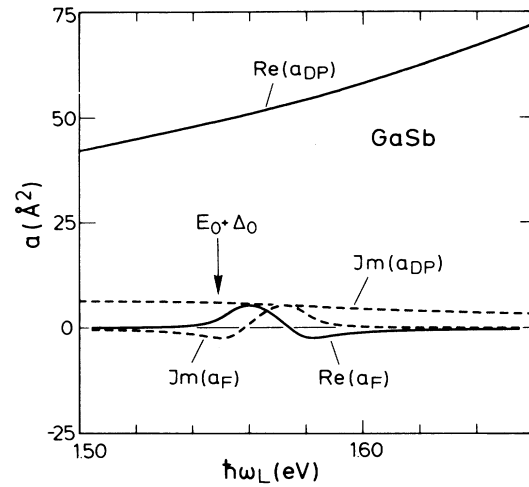


FIG. 3. Energy dependence of the Raman polarizabilities a_{DP} for LO-phonon-allowed and a_F for LO-phonon-intrinsic forbidden scattering as calculated for the fit of Fig. 1.

unreasonable deformation potentials d_0 below 15 eV. C_0'' of GaSb should not differ much from that of other III-V or IV-IV compounds. With the best value of C_0'' of GaAs ($C_0'' = 1.5$) (Ref. 33) or Ge ($C_0'' = 1.9$) (Ref. 33), d_0 amounts to about 23 and 18 eV, respectively. This value is still somewhat low when compared with 28–32 eV determined experimentally from the broadening of the $E_0 + \Delta_0$ gap following the analysis of Lawaetz³⁰ and evaluated from band-structure calculations ($d_0 = 32 \text{ eV}$).³¹

The parameter A_2 describing the contribution from the E_1 and $E_1 + \Delta_1$ gap can also be related to the corresponding two- ($d_{3,0}^5$) and three-band optical deformation potentials ($d_{3,0}^5$) (Ref. 34) by the expression (in atomic units, $e = \hbar = m = 1$):^{14,15,35}

$$A_2 = \frac{\sqrt{2}a_0}{9\pi E_1^2} \left[d_{3,0}^5 + \frac{1}{2\sqrt{2}} d_{1,0}^5 \right]. \quad (8)$$

In Eq. (8), a_0 is the lattice constant and E_1 is the energy of the E_1 gap. Equation (8) assumes $\hbar\omega_L - E_1$ to be large with respect to the spin-orbit splitting Δ_1 . The two-band deformation potential $d_{1,0}^5$ introduces only a small correction to $d_{3,0}^5$.¹⁵ From Eq. (8) and $A_2 = 50$ one obtains $d_{3,0}^5 + (1/2\sqrt{2})d_{1,0}^5 = 53 \text{ eV}$. This value is somewhat larger than those found in the literature for other materials such as Ge or InSb. For Ge pseudopotential calculations yield $d_{3,0}^5 = 41 \text{ eV}$ and $d_{1,0}^5 = -23 \text{ eV}$ (Ref. 36), $d_{3,0}^5 = 48 \text{ eV}$ (Ref. 37), or $d_{3,0}^5 = 40 \text{ eV}$ and $d_{1,0}^5 = -21 \text{ eV}$ (Ref. 38) at the L point $[(\pi/a_0)(1,1,1)]$ of the Brillouin zone. In the case of InSb, $d_{3,0}^5 = 38 \text{ eV}$ (Ref. 37) or $d_{3,0}^5 = 32 \text{ eV}$ and $d_{1,0}^5 = -14$ (Ref. 39) were calculated from pseudopotentials, whereas $d_{3,0}^5 = 33 \pm 8 \text{ eV}$ and $d_{1,0}^5 = -16 \pm 4 \text{ eV}$ were determined experimentally from the resonance of Raman scattering by LO phonons near the E_1 gap.⁴⁰ Thus, the values known for Ge yield $d_{3,0}^5 + (1/2\sqrt{2})d_{1,0}^5$ between 33–41 eV; those for InSb yield 27–33 eV. The experimental determination gives

$d_{3,0}^5 + (1/2\sqrt{2})d_{1,0}^5$ between 19–37 eV in InSb.

The sign of the interference determined by the relative sign of a_{DP} and a_F (Fig. 3) is the same as that found for GaAs (Ref. 8) and InP (Ref. 9), thus confirming that the deformation potential d_0 is positive, provided $s_e - s_h < 0$ holds in Eq. (9) of Ref. 10 (which should be the case according to $\mathbf{k}\cdot\mathbf{p}$ perturbation theory¹⁵) and the transverse dynamical charge e_T is positive on the Ga ion.²²

V. CONCLUSION

Measurements of the resonant Raman scattering by LO phonons and the interference between dipole-allowed and dipole-forbidden mechanisms in GaSb have been shown to provide accurate values for the $E_0 + \Delta_0$ gap energy and its

Lorentzian broadening, as well as an estimate of the optical deformation potentials d_0 , $d_{3,0}^5$, and $d_{1,0}^5$. Although these effects in GaSb behave in a way similar to InP and GaAs, they exhibit some specific features. The dipole-forbidden scattering by LO phonons is very weak. The \mathbf{q} -induced intrinsic Fröhlich scattering can be clearly observed by means of the interference with the corresponding dipole-allowed deformation-potential scattering. Only $(30 \pm 7)\%$ of the dipole-forbidden Raman scattering by LO phonons seems to be due to the intrinsic \mathbf{q} -dependent contributions in the bulk sample studied.

Note added in proof. The deformation potential $d_0 = 23.4$ eV has been recently calculated for GaSb with the linear-muffin-tin-orbital method (LMTO) by L. E. Brey, N. E. Christensen, and M. Cardona [Phys. Rev B (to be published)].

- ¹F. Cerdeira, W. Dreybrodt, and M. Cardona, *Proceedings of the Eleventh International Conference on the Physics of Semiconductors* (Polish Scientific Publishers, Warsaw, 1972), p. 1142.
- ²W. Dreybrodt, W. Richter, F. Cerdeira, and M. Cardona, *Phys. Status Solidi B* **60**, 145 (1973).
- ³R. L. Farrow, R. K. Chang, and R. M. Martin, in *Proceedings of the Fourteenth International Conference on the Physics of Semiconductors, Edinburgh*, edited by B. L. H. Wilson, Inst. Phys. Conf. Ser. No. 43 (IOP, London, 1978), p. 485.
- ⁴C. Tejedor, J. M. Calleja, F. Meseguer, E. E. Mendez, C.-A. Chang, and L. Esaki, *Phys. Rev. B* **32**, 5303 (1985).
- ⁵R. M. Martin, *Phys. Rev. B* **4**, 3676 (1971).
- ⁶R. Zeyher, *Phys. Rev. B* **9**, 4439 (1974).
- ⁷R. Zeyher, C.-S. Ting, and J. L. Birman, *Phys. Rev. B* **10**, 1725 (1974).
- ⁸J. Menéndez and M. Cardona, *Phys. Rev. B* **31**, 3696 (1985).
- ⁹J. Menéndez, M. Cardona, and L. K. Vodopyanov, *Phys. Rev. B* **31**, 3705 (1985).
- ¹⁰W. Kauschke and M. Cardona, *Phys. Rev. B* **33**, 5473 (1986).
- ¹¹A. A. Gogolin and E. I. Rashba, *Proceedings of the Thirteenth International Conference on the Physics of Semiconductors* (Tipografia Marves, Rome, 1976), p. 284.
- ¹²A. A. Gogolin and E. I. Rashba, *Solid State Commun.* **19**, 1177 (1976).
- ¹³J. Menéndez and M. Cardona, *Phys. Rev. Lett.* **51**, 1297 (1983).
- ¹⁴M. H. Grimsditch, D. Olego, and M. Cardona, *Phys. Rev. B* **20**, 1758 (1979).
- ¹⁵M. Cardona, in *Light Scattering in Solids II*, Vol. 50 of *Topics in Applied Physics*, edited by M. Cardona and G. Güntherodt (Springer, Heidelberg, 1982), p. 19.
- ¹⁶R. M. Lyddane, R. G. Sachs, and E. Teller, *Phys. Rev.* **59**, 673 (1941).
- ¹⁷H. C. Gatos and M. C. Lavine, in *Progress in Semiconductors*, edited by A. F. Gibson and R. E. Burgess (Temple, London, 1965), Vol. 9, p. 1.
- ¹⁸J. Wagner and M. Cardona, *Solid State Commun.* **48**, 301 (1983).
- ¹⁹W. C. Dash and R. Newman, *Phys. Rev.* **99**, 1151 (1955).
- ²⁰D. E. Aspnes and A. A. Studna, *Phys. Rev. B* **27**, 985 (1983).
- ²¹W. Kauschke, M. Cardona, and E. Bauser, *Phys. Rev. B* **35**, 8030 (1987).
- ²²W. A. Harrison, *Electronic Structure and Properties of Solids* (Freeman, San Francisco, 1980).
- ²³M. Reine, R. L. Aggarwal, and B. Lax, *Phys. Rev. B* **5**, 3033 (1972).
- ²⁴D. A. Hill and C. F. Schwerdtfeger, *J. Phys. Chem. Solids* **35**, 1533 (1974).
- ²⁵M. Reine, R. L. Aggarwal, and B. Lax, *Solid State Commun.* **8**, 35 (1970).
- ²⁶M. Cardona and G. Harbeke, *J. Appl. Phys.* **34**, 813 (1963).
- ²⁷R. R. L. Zucca and Y. R. Shen, *Phys. Rev. B* **1**, 2668 (1970).
- ²⁸P. B. Klein and R. K. Chang, *Phys. Rev. B* **14**, 2498 (1976).
- ²⁹N. N. Sirota and Gololobov, *Dokl. Akad. Nauk SSSR* **144**, 398 (1962).
- ³⁰P. Lawaetz, D. Sc. thesis, The Technical University of Denmark, Lyngby, 1978 (unpublished).
- ³¹A. Blacha, H. Presting, and M. Cardona, *Phys. Status Solidi B* **126**, 11 (1984).
- ³²P. Y. Yu, M. Cardona, and F. H. Pollak, *Phys. Rev. B* **3**, 340 (1971); P. Y. Yu, Ph.D. thesis, Brown University, 1972 (unpublished).
- ³³M. Cardona, in *Atomic Structure and Properties of Solids*, Proceedings of the International School in Physics "Enrico Fermi," Course 52, edited by E. Burstein (Academic, New York, 1972), p. 514; C. W. Higginbotham, M. Cardona, and F. H. Pollak, *Phys. Rev.* **184**, 821 (1969).
- ³⁴E. O. Kane, *Phys. Rev.* **178**, 1368 (1969).
- ³⁵A. K. Sood, C. Contreras, and M. Cardona, *Phys. Rev. B* **31**, 3760 (1985).
- ³⁶H. Presting, Ph.D. thesis, Universität Stuttgart, 1985 (unpublished).
- ³⁷M. Pötz and P. Vogl, *Phys. Rev. B* **24**, 2025 (1981).
- ³⁸M. A. Renucci, J. B. Renucci, R. Zeyher, and M. Cardona, *Phys. Rev. B* **10**, 4309 (1974).
- ³⁹H. Presting (private communication).
- ⁴⁰J. Menéndez, L. Viña, M. Cardona, and E. Anastassakis, *Phys. Rev. B* **32**, 3966 (1985).